

Blurred Lines: How Spatial Smoothing Influences the Statistical Analysis and Interpretation of fMRI Data

MSc Computational Neuroscience, Cognition and AI

Submitted by:

Lowri Powell
Student Number: 20158537

September 2024

University of Nottingham

Abstract

Functional magnetic resonance imaging (fMRI) is a widely used tool in neuroscience for mapping brain activity via the blood-oxygen-level dependent (BOLD) signal. Researchers acquire raw data from the scan and must conduct several preprocessing steps before statistical analysis in order to get meaningful and interpretable results. One such step is spatial smoothing, which involves blurring the data to reduce the signal to noise ratio (SNR). Spatial smoothing achieves this by averaging the value of voxels with neighbours across a given region of space, which also enhances the detection of neuronal activations. A larger region of smoothing increases the signal to noise ratio, but at the cost of spatial resolution. The loss of spatial resolution has the potential to cause blurring between distinct activation patterns and obscuring the finer anatomical details. However the extent to which this happens is not widely known. This study uses a 7T, high spatial resolution scanner to collect raw data from a simple visual stimuli paradigm. Participants were presented with either faces or objects but didn't have to produce a reaction. Then preprocessing was conducted as usual, however systematically varied the Full Width Half Maximum (FWHM) values for spatial smoothing. Then the different conditions were subjected to parametric analysis and visualisation scrutiny. The study found that there were differences in average number of clusters, the cluster size, the size variance, and also the peak activation coordinates for the top clusters. The study suggests that the extent of spatial smoothing can have a large impact on statistical analysis. Whilst the results of a study might not be obscured into inaccuracy, it is still an important factor for researchers to consider when conducting neuroimaging studies.

Contents

Contents	1
1 Introduction	1
1.1 Preprocessing fMRI Data	2
1.2 Spatial Smoothing	2
1.3 Alternatives to Gaussian Filtering	3
1.4 Impact on statistical analysis and interpretation	5
1.5 Experimental Objectives and Rationale	5
2 Methodology	6
2.1 Participants	6
2.2 Experimental Protocol	6
2.3 Image Acquisition	6
2.4 Image Analysis	6
3 Results	8
3.1 Statistical Analysis	8
3.2 Interpretation of Data	9
4 Discussion	14
4.1 Interpretation of Results	14
4.2 Implications of Results	16
4.3 Limitations of the Study	17
4.4 Further Research	17
4.5 Conclusion	17

1 Introduction

Functional magnetic resonance imaging (fMRI) is a prevailing non-invasive technique for investigation into brain function and cognitive processes. By measuring changes in blood flow it provides insights into the workings of the cortex (Bandettini et al., 1992). The principles behind fMRI are based on the correlation between cerebral blood flow and neuronal activation (Buxton et al., 1998). When neurons in a brain region becomes more active, it requires more oxygen and thus demands an increase in oxygenated blood to that region (Logothetis et al., 2001). Haemoglobin is the molecule within blood which is responsible for carrying oxygen around the bloodstream. As it carries oxygen and deposits it in various wanting regions, its magnetic properties change (Ogawa et al., 1992). fMRI utilises this change in magnetic properties governed by its oxygenated state to produce a blood-oxygen-level dependent (BOLD) signal. This BOLD signal is what fMRI uses to indirectly measure the areas of the brain with heightened neural activity (Kwong et al., 1992). The MRI scanner gathers the BOLD signal data across the whole brain over a certain time frame, which is then processed to create the functional brain maps which show the location of active brain regions. This technique has been used to determine the effects of medication within pharmacological studies (Wandschneider & Koepp, 2016), to diagnose and asses various different conditions such as cochlear implants, seizure disorders and brain tumours (Bartsch et al., 2006). Whilst fMRI can be used in a vast number of fields, it is imperative to psychology and cognitive neuroscience.

Its contributions towards understanding localisation of function within the brain has been monumental in moving the field forward.

1.1 Preprocessing fMRI Data

Similar to how manuscripts need editing and drafting before becoming a novel, researchers must process the raw data from an MRI scanner to create tangible results. The essence of these preprocessing steps is quality control and preparation for statistical analysis. It involves cleaning the data from artefacts made by the scanner, the participant, or the researcher, and allowing the data to be fit for statistical assumptions.

Preprocessing can be conducted in a variety of ways, and using a range of software such as SPM and FSL. Whilst the distinct processing steps can differ across the domain, researchers tend towards a standard routine of preprocessing steps (Poldrack et al., 2011). This process starts with slice timing, where each slice of data is aligned to the same time point. This is to account for the staggered acquisition times which happens during the scanning session (Sladky et al., 2011).

Slice timing is followed by realignment, sometimes referred to as motion correction. This addresses the confounds of any movements which the participant may have made when in the scanner during the study. It typically uses the first scan as a reference image and transposes the subsequent scans to align with that image (Friston et al., 1996).

Segmentation is then done to separate grey matter, white matter and cerebrospinal fluid to improve the accuracy of the subsequent analysis (Ashburner & Friston, 2005). The BOLD signals acquired in the scan typically only refer to grey matter as it is well documented that it corresponds to neuronal activity (Rauch et al., 2008). The activity within white matter and cerebrospinal fluid are less well understood so therefore segregated (Gawryluk et al., 2014; Schilling et al., 2023).

The final step in preprocessing tends to be spatial smoothing, this is critical for removing any noise in the data which is inherent to fMRI scanning. Spatial smoothing aims to improve the signal to noise ratio (SNR), and also enhance the detectability of brain activity prior to statistical analysis (Mikl et al., 2008). The technique is similar to that done in other forms of image processing, where images collected are blurred slightly through a chosen low-pass filter method. By sending the image through the low pass filter, it reduces the amount of high-frequency noise and increases the statistical power of the analysis. This makes it easier to distinguish regions of the brain that are significantly more active from random noise (Worsley et al., 1996). The main goal of spatial smoothing is to reinforce the true signals of consistent brain activity whilst minimising fluctuations caused by noise.

1.2 Spatial Smoothing

A conventional technique for spatial smoothing involves using a Gaussian kernel to convolve over the brain data and average voxel values with their neighbours. The size of this kernel is determined by the shape of the Gaussian. The Gaussian equation is given by:

$$G(x) = \frac{1}{\sqrt{2\pi\sigma^2}} \exp\left(-\frac{x^2}{2\sigma^2}\right),$$

Where σ represents the standard deviation, this governs the spread of the data, changing the dynamic of the kernel. But within preprocessing, the kernel is not directed by sigma, but a Full Width at Half Maximum (FWHM) parameter which has a direct relationship with σ . FWHM is known as the distance between two points on the Gaussian curve where the value is half of its peak (Figure 1a). Image pixels, or voxels in fMRI cases, between these FWHM boundaries are averaged, and any pixels outside the boundaries are not. This FWHM is used over σ as it is more intuitive to understand the extent of

blurring as it tells you how many millimetres are blurred together. The relationship between σ and FWHM is

$$\text{FWHM} = 2\sqrt{2 \ln(2)}\sigma \approx 2.355\sigma.$$

As FWHM is directly proportional to σ , a larger FWHM leads to a larger σ . This greater σ makes the Gaussian curve more broad and shorter (Figure 1b). This wide kernel will reach over a larger portion of the data and results in a higher degree of blurring within the image. A larger kernel increases the detectability of weak signals and removes a greater portion of noise (Worsley, 2001), but it also decreases the spatial resolution of the data. In an fMRI dataset, a larger kernel would blur over more activation patterns and merge regions of activity.

To illustrate the impact of varying FWHM values, Figure 2 presents a standard MNI brain map demonstrating how different FWHM values affect the data its given. A FWHM of 0mm indicates no spatial smoothing at all, and whilst the image is not finely detailed, it is easy to discriminate the different regions of the brain, and its sulci and gyri are easily seen. With a 3mm FWHM, there is already a loss of the finer details of the image, the topology of the brain is slightly harder to distinguish but there are still boundaries which are clear and regions are identifiable. However, when the FWHM is at 6mm, the amount of detail lost is clear. The skull is still easy to see, however the grooves and ridges of the cortex are barely detectable. This is what happens to the data under Gaussian filtering in order to reduce noise and increase signal detectability.

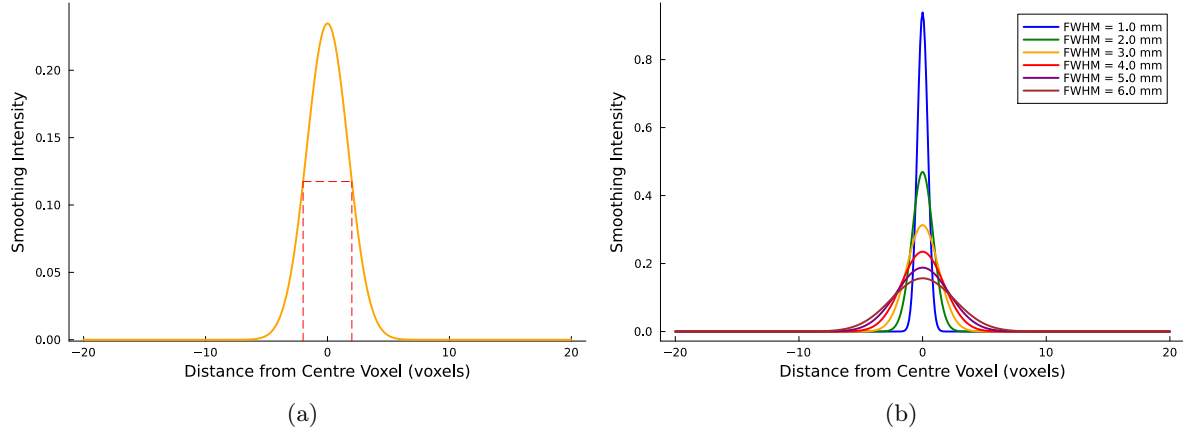


Figure 1: Gaussian and how the FWHM affects the kernel shape

1.3 Alternatives to Gaussian Filtering

While the greater portion of fMRI studies use this Gaussian filtering method with FWHM to conduct their spatial smoothing, there are other, perhaps more sophisticated techniques available. Anisotropic diffusion, also known as Perona-Malik diffusion (Perona & Malik, 1990) is a technique which can reduce the SNR whilst still maintaining some key characteristics of the data, such as boundaries and edges, which are crucial for interpretation. This method works by iteratively updating voxel-based values based on a diffusion process which can vary in different directions. It uses partial differential equations to diffuse the image in regions with low gradients, for example in a homogeneous region of the brain, whilst simultaneously inhibiting diffusion across edges. Essentially, if there is a sudden drop off in signal as it reaches a boundary, it will not average over it. The diffusion is driven by a conductance function, which decreases as the gradient magnitude increases, as it would when you approach an edge. This means diffusion is slower across stronger edges, like changes in matter within the brain, and faster within the

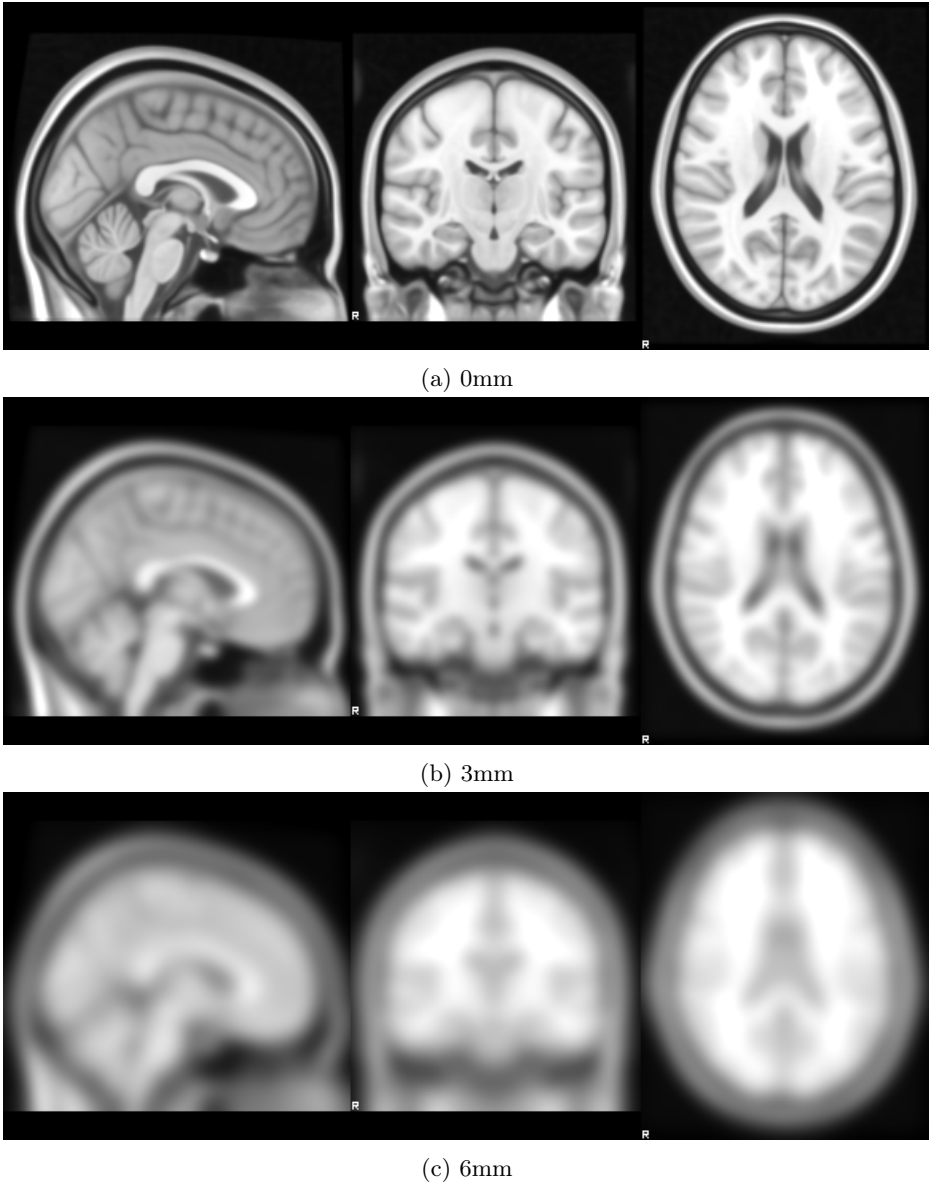


Figure 2: The reality effect of spatial smoothing on a standard MNI brain.

same region of the brain. Whilst anisotropic diffusion is better for the preservation of structural detail and preventing edge blurring, it is a lot more computationally demanding. Gaussian filtering is much simpler and more efficient by uniformly averaging voxels to blur the image.

A similar technique which preserves edges while blurring is bilateral filtering. This is a non-linear smoothing filter which can maintain the boundaries within an image or dataset (Tomasi & Manduchi, 1998). It preserves boundaries by averaging pixel values based on their spatial proximity to one another and similarity in signal strength. This means that voxels close by with similar intensities contribute more to the final value than another nearby voxel with a very different signal strength would. As a result bilateral filtering allows for the removal of noise and maintains sharp details. Yet once again, this technique requires a significant computational load, which allows Gaussian filtering to be the more attractive method in most studies. Whilst edge preservation methods such as anisotropic diffusion and bilateral filtering offer undeniable advantages in reducing the loss of spatial resolution in spatial smoothing, their higher computational cost and complexity mean they forfeit to the traditional and more simple method of Gaussian filtering. Gaussian filtering has remained as the preferred choice of

smoothing techniques for many years and is well established within many statistical analysis toolboxes. Yet it is important to note the rise of the more complex and refined methods which help to reduce such a problem inherent to spatial smoothing.

1.4 Impact on statistical analysis and interpretation

Despite its faults spatial smoothing is critical for neuroimaging studies. One characteristic is it controls the amount of false positives being reported. As the extent of smoothing increases, the SNR improves, which means that there is less noise potentially being reported as real activation. This increases the statistical power of a study, but the region which is determinedly active is less well defined.

Additionally, spatial smoothing is key for group-level analysis. Within a study there might be multiple participants, it could only be small sample or it could be an extremely larger scale study with hundreds of participants. Within these samples, each brain will exhibit anatomical variation due to genetics and environment, leading to problems with individual differences. Spatial smoothing helps to reduce these confounds by blurring through any differences in brain space. These characteristics make it difficult for researchers to find an equilibrium between enhancing SNR and maintaining spatial specificity.

Although the effect of spatial smoothing on images is understood, its impact on statistical analysis and data interpretation is even more critical to the field of cognitive neuroscience. As discussed previously, a higher value of FWHM leads to a higher proportion of blurring within the image. This lays the groundwork for understanding how spatial smoothing affects the statistical analysis and visualisations of active brain regions. Researchers may grasp the fundamental changes spatial smoothing introduces to the data, but its more subtle effects on analysis and the interpretation of results might not be fully recognised.

1.5 Experimental Objectives and Rationale

The aims of this study were to understand how spatial smoothing directly impacts statistical analysis and further interpretation of fMRI data. To accomplish this, the well-documented paradigm of localisation of face processing was used. The faces vs objects processing phenomena is extremely robust at exposing regions of the brain significantly more active to one of the stimuli than the other. The fusiform facial area (FFA) is designated to processing any faces we see on a day-to-day basis, whereas the Lateral Occipital Cortex (LOC) is recognised as the region responsible for object recognition (Kanwisher et al., 1997). By using this paradigm, the study exploited the differences in activations between the regions to examine how spatial smoothing changes the results.

Coupled with such a robust experimental design, the study also used a 7T MRI scanner, with a superior spatial resolution. This will be fundamental in understanding what effect varying the levels of spatial smoothing will have on more delicate regions of the brain. The higher resolution, reduced partial volume effects (Newton et al., 2012), and improved contrasts are expected to produce clearer and more accurate data than a 3T scanner. This advanced imaging capability was crucial for thoroughly appreciating how different intensities of spatial smoothing might affect the statistical analysis and further interpretation of the data.

The method and extent of spatial smoothing is not standardised within fMRI studies (Borowsky et al., 2013; Dehghani et al., 2023; Fox et al., 2009; Weiskopf et al., 2004) but a typical FWHM value used within large scale studies is around 8mm. This is because each study will require a different level of spatial smoothing dependent on its experimental design. Researchers are expected to select an appropriate level and disclose this within the article for the field to compare to, however this does not always happen in a uniform manner which allows other researchers to compare their results to (Dymarkowski et al., 1998; Passarotti et al., 2003).

The overall goal of this study was to give researchers an insight into what is happening when they are preprocessing their data and what consequences it might have on their results. By appreciating the complexity of spatial smoothing, this study hopes to make the process of choosing a spatial smoothing level more involved than it might previously have been.

2 Methodology

2.1 Participants

The study included one participant, an employee at the Sir Peter Mansfield Imaging Centre, University of Nottingham. This single participant was involved to verify the proper setup of the scanner following its installation at the centre.

2.2 Experimental Protocol

The experimental protocol involved a passive viewing task where the participant was presented with images of faces or objects. Each trial consisted of a 24-second cycle, beginning with 12 seconds of rest, followed by 12 seconds of face presentation, another 12 seconds of rest, and 12 seconds of object presentation. This cycle was repeated for a total of 10 blocks. During the task, the participant was not required to make any overt responses.

2.3 Image Acquisition

Functional and structural MRI data were acquired using a Phillips Acheiva with a magnetic field strength of 7T in the Sir Peter Mansfield Imaging Centre at the University of Nottingham. Functional images were obtained using an echo-planar imaging (EPI) sequence with the following parameters: repetition time (TR) of 2000 ms, echo time (TE) of 25 ms, and a flip angle of 68 degrees. Each functional volume consisted of 32 slices with a slice thickness of 1.499885 mm, covering the whole brain. The voxel size was $1.432 \times 1.432 \times 1.499885 \text{ mm}^3$, with a field of view (FOV) of $183.296 \times 183.296 \times 47.996 \text{ mm}$ and a matrix size of $128 \times 128 \times 32$ voxels. A total of 120 volumes were acquired per run, with each scan session lasting approximately 240 seconds (4 minutes).

Structural images were acquired using a phase-sensitive inversion recovery (PSIR) sequence (Mougin et al., 2010) with the following parameters: TR = 6.3 ms, TE = 2.62 ms, and a flip angle of 5 degrees. The voxel size for structural imaging was $0.677 \times 0.677 \times 0.7 \text{ mm}^3$, with 320 x 320 voxels in-plane and 224 slices. Stimuli were presented using a projector, and the participant's head was secured with foam padding and a head coil to minimise movement during scanning.

2.4 Image Analysis

Functional MRI data processing was carried out using FEAT (fMRI Expert Analysis Tool) version 6.00, part of FSL (FMRIB's Software Library www.fmrib.ox.ac.uk/fsl). The following pre-statistics process was applied; motion correction using MCFLIRT (Jenkinson et al., 2002); spatial smoothing was varied from 0mm to 6mm (inclusive) with 1mm increases; grand-mean intensity normalisation of the entire 4D dataset by a single multiplicative factor; highpass filtering temporal filtering (Gaussian-weighted, least squares straight line fitting, with sigma = 24.0s). Time-series statistical analysis was carried out using FILM with local auto-correlation (Woolrich et al., 2001). Z (Gaussianised T/F) statistics images were thresholded using clusters determined by $Z > 3.1$ and a (corrected) cluster significance threshold of $P = 0.05$ (Worsley, 2001). Four contrasts were defined faces, objects, faces>objects and objects>faces,

but for the purposes of this study, only contrast 3 (faces > objects) will be used in the results section. This contrast was selected to clearly distinguish the neural responses associated with face processing compared to object processing, thereby providing a focused examination of the hypothesis.

A high-pass filter with a 100 second cutoff was selected to remove low frequency drifts (Smith et al., 1999) whilst preserving the higher frequency components related to brain activity. Motion correction was applied with MCFLIRT to account for any head move artefacts that could confound the effects of smoothing. This uses the middle volume as a reference and aligns each volume to this. B0 warping was not applied as the magnetic field distortions were deemed minimal in a one participant, one scan study. However it is noted that neglecting this step might influence the spatial characteristics of the study. Again, slice time correction was not implemented within preprocessing as it was assumed to be not critical for a single participant study. Brain extraction through BET was also turned off, allowing non-brain tissue to be considered within the analysis, which again could impact the results as it might introduce extraneous signals. Intensity normalisation was also not performed, recognising that variations in the signal intensity might influence results though the risk in a single scan study with a sole participant was decided to be low. Finally, spatial registration was not applied, this was to ensure that the data was in a consistent space prior to smoothing.

Ultimately the aim of this study was to understand how spatial smoothing influences the statistical analysis, therefore the other preprocessing steps were seen as confounds to the results. As spatial smoothing is known to decrease spatial resolution, the influence of the other preprocessing steps on the data were to be avoided to uncover the true influence of smoothing alone.

Once the data had been preprocessed, simple analysis techniques were used to understand how spatial smoothing had transformed the data. For each condition of FWHM the descriptive statistics were collected for the number of clusters, their sizes, and the standard deviations (SD), this was done using FSL command line tools such as 'fslmaths'. Cluster coordinates were found using similar shell commands and the top 5 clusters were decided upon by the z-score. Figures were created using Python, MATLAB and Julia. Additionally, to measure how far the peak activation coordinates of clusters had travelled, the Euclidean distance for each of the top five clusters in each FWHM condition will be compared to a baseline coordinate. The coordinate with the highest activity for the 6mm FWHM condition was used as a baseline, and the coordinates for all other conditions were measured relative to this baseline. This was chosen as baseline because 6mm has fewer clusters, so would encapsulate the numerous other clusters that might be seen at lower smoothing levels. This distance is taken as

$$\text{Distance} = \sqrt{(x_1 - x_2)^2 + (y_1 - y_2)^2 + (z_1 - z_2)^2}$$

where (x_1, y_1, z_1) is the baseline coordinate, and (x_2, y_2, z_2) is the coordinate to which baseline is being measured.

As part of the aim of this study investigating how spatial smoothing changes the data, it is important to measure how similar the clusters are. To do this each spatial smoothing level was compared to another and the Dice-Sørensen Coefficient was used (Dice Coefficient). This is a statistical test to quantitatively determine how similar two volumes are (Dice, 1945; Sørensen, 1948). The value of this coefficient varies from 0 to 1, low values indicate dissimilar samples, a value of 1 indicates identical samples (Figure 3). The original method found the ratio between the intersect of two sets of data and the sum of each of the datasets in the following equation:

$$\text{DSC} = \frac{2 * A \cap B}{A + B}$$

This has been used in neuroimaging for decades (Rombouts et al., 1997), and will help to explain the similarities in the clusters shape and area. There is an expected dissimilarity between the clusters

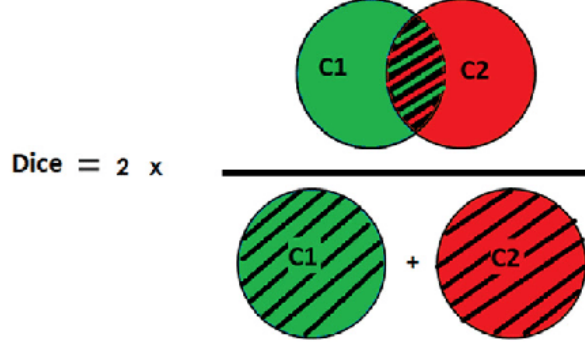


Figure 3: Diagram of the Dice Coefficient equation showing the intersection of A and B

as noise is removed and spatial resolution lost, however the exact trend is worth noting.

3 Results

3.1 Statistical Analysis

Once preprocessing was complete, the descriptive statistics of the datasets were collected. These results are summarised in Table 1 and include the number of voxels, the average size of the voxels, and their standard deviations (SD).

FWHM (mm)	Number of Clusters	Mean Cluster Size (voxels)	SD (voxels)
0	263	33.265	198.06
1	101	115.265	519.135
2	71	184.014	657.987
3	31	532.438	1320.38
4	23	821.833	1839.47
5	16	1211.35	2368.91
6	11	1841.33	3126.46

Table 1: Descriptive statistics for each FWHM conditions.

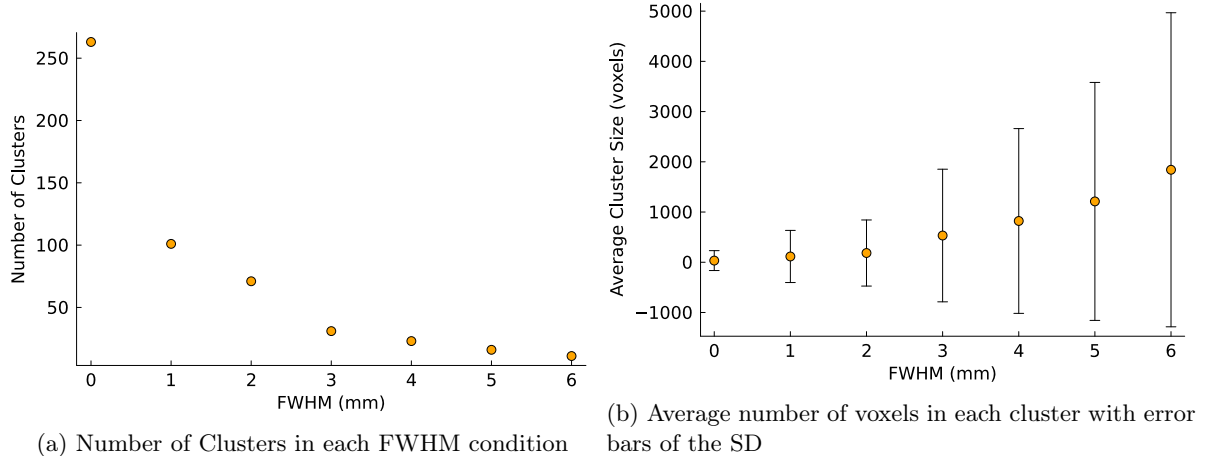


Figure 4: Graphs of the descriptive statistics for each FWHM condition

From the Figure 4a we can see that as FWHM increases, the number of clusters decreases. This is intuitive as when blurring across a larger space, the smaller clusters will merge. The 263 clusters that

are active in the 0mm FWHM condition are collected in a similar anatomical space in the 11 larger clusters observed in the 6mm sample. The difference in the number of clusters decreases as FWHM increases, indicating that smaller smoothing levels have a larger impact on the data, while higher levels of smoothing result in diminishing changes.

Figure 4b shows that as FWHM increases, the average cluster size also increases, as does its SD. With no spatial smoothing, the average size of the clusters is just 33 voxels, which increases considerably to 1841 when there is 6mm of spatial smoothing. Therefore a wider spatial smoothing kernel will encapsulate more voxels into the clusters than no spatial smoothing, reducing noisy data. However, the larger spatial smoothing means that the voxels are less likely to be erroneous. The SD also increases as more spatial smoothing is applied, meaning that as FWHM increases, clusters not only grow larger, but they also vary more in size. This indicates that spatial smoothing causes greater variability in cluster sizes, likely due to the irregularities in the merging of differently sized clusters. Some small clusters will be fully absorbed by larger ones, whilst others might expand disproportionately. This trend suggests that higher values of FWHM lead to more pronounced blurring as expected nearby clusters are aggregated and there is more variability in their sizes.

3.2 Interpretation of Data

The analysis of peak activation coordinates across varying FWHM levels reveal notable trends in activation patterns (Table 2). For instance, the coordinate (99, 22, 4), or its neighbour (100, 22, 4) appears to be a top 5 active coordinate in all FWHM values except in the 6mm condition. This indicates that this location is a seemingly robust centre for activation. However, the z-scores associated for this coordinate changes with FWHM, for example in 0mm, (99, 22, 4) has a z score of 11.5. The results show that the coordinates shift slightly with increased FWHM, illustrating how smoothing affects the localisation of peak activations.

To assess the impact of spatial smoothing on the localisation of peak activations, Euclidean distances were calculated between the top coordinates of each FWHM condition and the baseline coordinate from the 6mm FWHM condition (Table 3). This table shows that there is seemingly no apparent order to how the activation coordinate changes from baseline, however there seems to be some similarities in the distances when plotted (Figure 5). The graph implies that the distances seem to gather around three points. One being the baseline, with only 1mm FWHM not having a close distance in its top five coordinates. The other two are around between 50-60 voxels and 90 voxels away. Whilst the Euclidean distances is considered in all 3 dimensions, it cannot be certain that they refer to the same coordinate by itself, but intuitively it could imply that there are 3 “hotspots” of activation and the peak coordinate lies somewhere within them for any of the FWHM conditions.

To understand how similar the clusters were, the Dice Coefficients were calculated for all combinations (Figure 6). As conditions move towards larger FWHM values, the Dice coefficients generally increase. For instance, the similarity between 0mm and 6mm is 0.3538, which is lower compared to the similarity between 5mm and 6mm, which is 0.9111. This is expected as larger changes in blurring would change the data to a greater extent. Moreso, the Dice coefficients for the early conditions (0mm to 2mm) are relatively lower. This indicates that conditions with smaller FWHM values have less similarity compared to conditions with larger FWHM values. For example, the similarity between 0mm and 2mm is 0.6968, while the similarity between 5mm and 6mm is 0.91. This implies that as the extent of spatial smoothing increases, there is little difference been explicit values.

The analysis of functional maps across varying FWHM values (Figure 7) reveals several important insights into how spatial smoothing affects the presentation of fMRI data. At 0mm FWHM (Figure 7a), the data are highly granular and noisy, with no spatial smoothing applied. This results in a cluttered

Table 2: Top Brain Coordinates and Z-Scores for Different FWHM Values

FWHM (mm)	Coordinates	Z-Score
0	(99, 22, 4)	11.5
	(19, 33, 16)	9.64
	(34, 46, 1)	9.42
	(36, 83, 30)	9.31
	(93, 18, 9)	8.82
1	(99, 22, 4)	10.2
	(36, 42, 2)	8.96
	(94, 29, 1)	7.92
	(93, 19, 10)	7.77
	(18, 33, 16)	7.75
2	(99, 22, 4)	11.6
	(32, 48, 1)	10.4
	(36, 32, 1)	9.08
	(19, 33, 16)	8.99
	(36, 83, 30)	8.9
3	(34, 45, 1)	10.8
	(99, 23, 4)	10.3
	(34, 83, 31)	8.57
	(103, 29, 16)	8.4
	(18, 33, 16)	7.81
4	(34, 45, 1)	9.83
	(100, 22, 4)	9.79
	(103, 29, 16)	8.35
	(33, 83, 31)	8.21
	(36, 33, 1)	6.9
5	(100, 22, 4)	8.94
	(34, 45, 1)	8.83
	(35, 83, 30)	8.43
	(41, 105, 0)	6.27
	(18, 51, 18)	5.83
6	(35, 83, 30)	8.13
	(33, 46, 1)	7.95
	(35, 39, 28)	5.43
	(78, 6, 6)	5.43
	(63, 88, 30)	5.19

and less interpretable map where activation patterns are difficult to discern due to the overwhelming presence of noise. In contrast, as FWHM is increased, particularly at 6mm (Figure 7c), the data exhibit significant blurring. This higher level of smoothing causes activation clusters to merge and spread across anatomical features such as sulci and gyri, leading to a distortion of the brain’s true shape. The blurring effect at this level of smoothing compromises the ability to accurately localise and interpret activation patterns, as clusters lose their distinctiveness and anatomical specificity. In between these extremes, the 3mm FWHM condition (Figure 7b) appears to offer a more balanced approach. This level of smoothing effectively reduces noise while preserving the overall topology of the brain. The clusters generated with 3mm smoothing retain a more accurate representation of brain anatomy, with less blurring of features compared to higher smoothing levels.

FWHM(mm)	Cluster	Distance
0	1	92.16
	2	54.33
	3	47.02
	4	1.00
	5	89.61
1	1	92.16
	2	49.66
	3	85.08
	4	88.66
	5	54.64
2	1	92.16
	2	45.55
	3	58.68
	4	54.33
	5	1.00
3	1	47.81
	2	91.50
	3	1.41
	4	87.95
	5	54.64
4	1	47.81
	2	92.85
	3	87.95
	4	2.24
	5	57.81
5	1	92.85
	2	47.81
	3	0.00
	4	37.68
	5	38.17

Table 3: Table showing the Euclidean Distance from the "baseline" coordinate

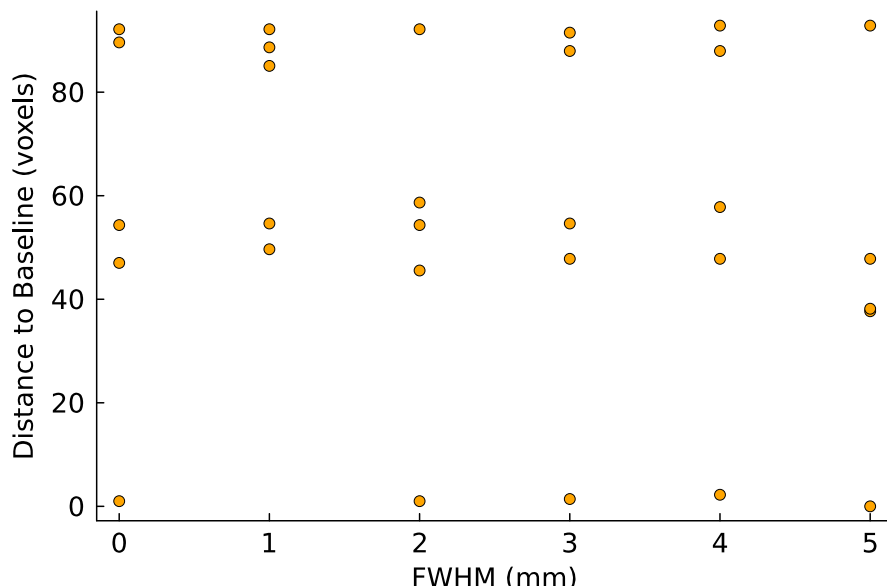


Figure 5: The Euclidean distance of each of the top 5 peak activation coordinates of the FWHM variables compared to the peak activation coordinate for 6mm FWHM

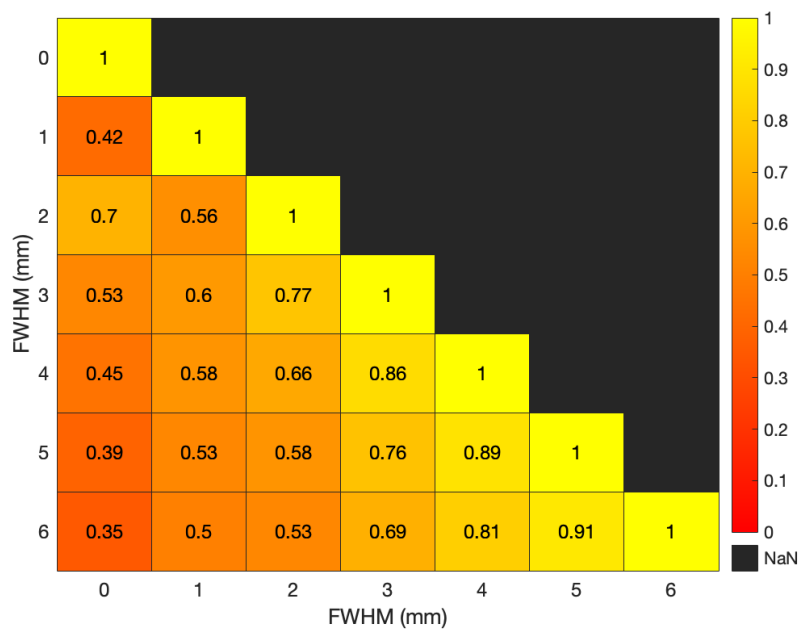
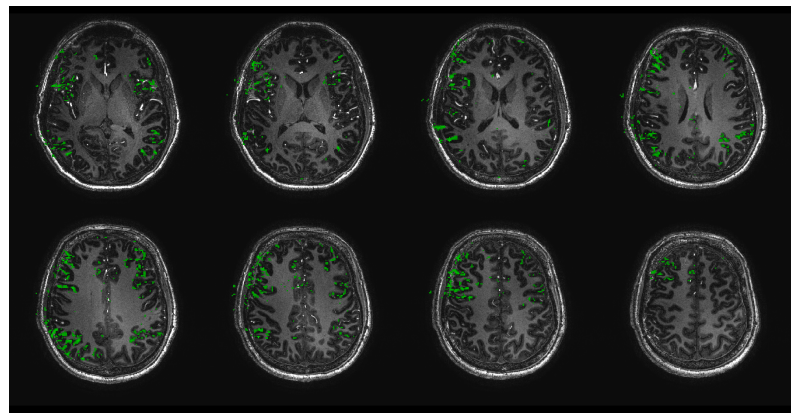
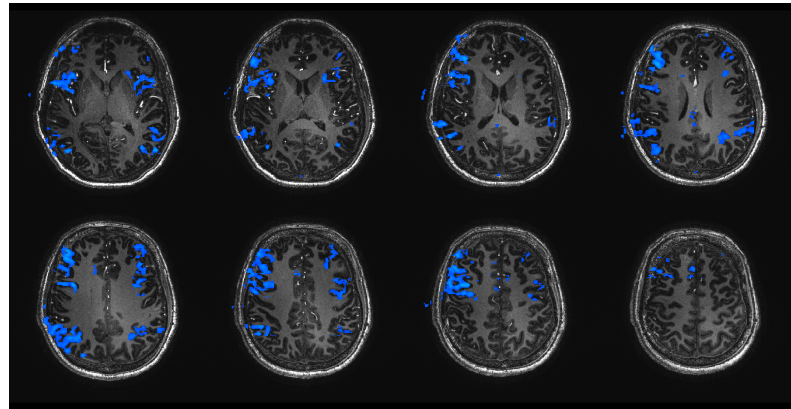


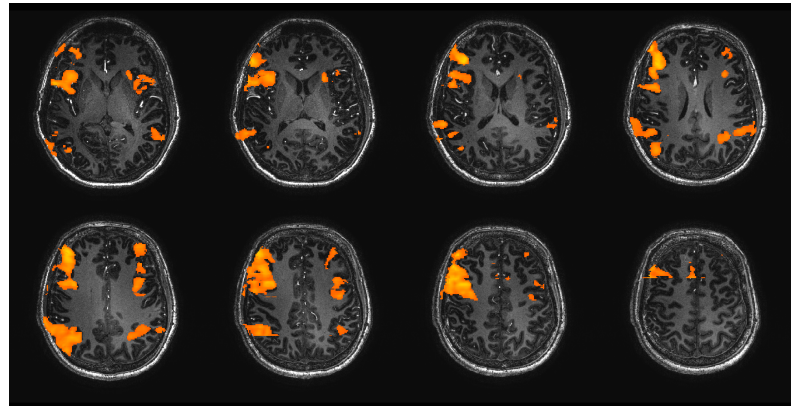
Figure 6: Matrix showing the Dice Coefficients for each FWHM compared to another



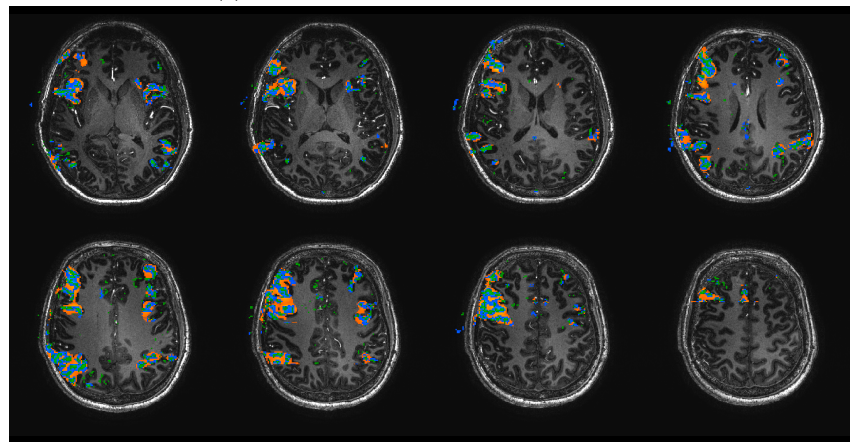
(a) Activation Clusters at FWHM 0mm.



(b) Activation Clusters at FWHM 3mm.



(c) Activation Clusters at FWHM 6mm.



(d) Overlay of FWHM 0mm, 3mm, and 6mm.

Figure 7: Comparison of Activation Clusters across Different FWHM Values.

4 Discussion

The data presented in this study indicates that spatial smoothing does affect the statistical analysis and interpretation of fMRI data. Whilst this change might not be detrimental to the overall conclusions of studies, there are nuanced changes that researchers should be aware of when conducting preprocessing.. Smoothing changes the description of clusters, removes finer details from cognitive processes, and moves the peak activation coordinate for significant clusters. These are all alterations which researchers should be aware of when comparing to previous literature, and in selecting their own processing conditions.

4.1 Interpretation of Results

The descriptive statistics given show that changing the FWHM changes the number of clusters, their size, and their variability in size. This change is intuitive, but still dramatic.

The results show that as the FWHM increases, the number of clusters in the dataset decreases. This is expected, as a larger kernel causes more data to be blurred in a given region, leading to the merging of more voxels. For example, an unsmoothed region with four clusters might merge into a single cluster after spatial smoothing. The initial sharp drop in cluster count followed by levelling-off suggests that increasing the FWHM leads to a saturation point. At higher FWHM levels, changes have less impact, whereas early stages of smoothing show a more pronounced effect. This could be due to sufficient noise removal, where clusters have merged to the extent that no smaller ones remain to absorb. At lower FWHM values, noise is more prominent, so smoothing has a stronger effect on reducing it. However, once noise is minimised, further smoothing mainly merges clusters. While smoothing reduces noise, higher levels can result in a loss of specificity, making it harder to localise brain activity. When this effect levels off, it may indicate that the data has reached a point where further loss of detail no longer significantly alters the results. This suggests there may be an optimal FWHM range for noise reduction and cluster detection, beyond which additional smoothing is unnecessary or even counterproductive. It is unclear how many is the “perfect” number of clusters, to have within an fMRI study, and there is a wide variety of research even outside of the field trying to understand how many is most appropriate for the given data (Dubes, 1987; Seghier, 2018; Windham, 1981; Zhou et al., 2014). This analysis directly supports the research aim by highlighting how spatial smoothing impacts the statistical analysis of fMRI data, specifically by altering the number of detectable clusters and potentially affecting the precision and accuracy of brain activity localisation

As FWHM increases, the average size of the clusters also increases. This is again due to more voxels being averaged over with a larger kernel and becoming part of clusters. Given the example of 4 individual clusters being merged at higher blurring levels, the four separate clusters might be 4 regions which contribute different things to cognitive process, however in a higher spatial smoothing level they are merged and deemed as one. This conflates the regions of activity in the brain as gaps in between clusters at lower levels are deemed as part of an active cluster at higher levels. This exposes another method in which spatial smoothing affects the statistical analysis of fMRI data. Liu et al. (2017) provides a theoretical explanation for this phenomenon from the perspective of correlation scale invariance. Their research demonstrates that spatial smoothing reduces noise in fMRI data, which in turn smooths the temporal correlation (tcorr) map, leading to an overestimation of activation spots in the neuroactivity clusters. They found that increased spatial smoothing can artificially expand the spatial extent of functional activation, suggesting that a more conservative smoothing kernel, such as one with a FWHM of no more than two voxels, is preferable for accurate correlation-based functional mapping. However, implementing this approach across all fMRI datasets would be challenging due to the various difficulties inherent in each dataset.

Several inherent characteristics of fMRI data present significant challenges when it comes to clustering and determining the appropriate spatial smoothing value (Thirion et al., 2014). These challenges include the sheer volume of data points (voxels) in a typical fMRI dataset, the inherently low signal-to-noise ratio (SNR), and the fact that only a small portion of voxels are likely to be functionally relevant. Additionally, artefacts, outliers (such as those caused by head movements or signal loss), and the complexity of brain activation patterns further complicate the choice of an optimal spatial smoothing parameter.

As FWHM increases, there is a notable increase in the SD of cluster sizes, which could be a product of several different causes. One is that the increase in SD reflects genuine variability in cluster sizes and brain activation regions. Larger FWHM values smooth over more voxels and potentially blend different activation patterns into larger, more variable clusters, suggesting diverse patterns of activation within the brain regions being merged into these large clusters. However, larger FWHM can also increase sensitivity to low-frequency noise, which has been characterised as a significant challenge in fMRI analysis (Tong et al., 2019). While smoothing is effective at removing high-frequency noise, it allows low-frequency noise to become more apparent, affecting the consistency of clusters across the dataset. This could result in larger clusters with more variability. Low-frequency noise can occur from sources such as physiological noise or the scanner itself. As spatial smoothing removes high-frequency noise and allows lower frequency signals to appear stronger, it could also be promoting low-frequency noise. This provides further insight into the influence that spatial smoothing has on data.

As shown in the results, the peak activation coordinate for the most significant clusters changes as the FWHM is changed. Whilst there is some continuity of these coordinates, the resettlement might suggest that FWHM disrupts the interpretation of significantly activated brain regions during a task and has been suggested in previous literature (Ball et al., 2012). Whilst the peak coordinate itself is not vital to drawing conclusions from studies, it could be important when comparing results across the literature. Having different activation centres for clusters between studies for the same cognitive process may confuse the understanding of cognition, when it is merely an artefact of the preprocessing stage. As the FWHM increases, the peak activation coordinates might shift because of this distortion, merging clusters or pushing the peak toward a region of stronger signal, even if it isn't truly the most activated area. This is directly related to the concerns raised about inflated false positive rates in fMRI, where smoothing can mask the true underlying neuronal signals (Cox et al., 2017; Eklund, Nichols, & Knutsson, 2016; Eklund, Nichols, & Knutsson, 2016). Again, spatial smoothing has been shown to change fMRI data in a way which could alter subsequent interpretation of results.

The Dice coefficients show that as FWHM increases, the effect that FWHM has on changing the cluster shape decreases. The sharper rise in values in the smaller spatial smoothing values could be explained by the removal of noise, like spatial smoothing intends on doing. The dissimilarity between the lower levels suggests that only a small FWHM is needed to remove a large portion of noise, further implying that there is an optimal level of FWHM that removes enough noise, whilst not blurring too much and destroying spatial accuracy. This trend in data highlights key points where fMRI data is transformed under spatial smoothing.

Viewing the functional maps shows the most intuitive way to understand how FWHM changes the data. At very low levels, the data is noisy, and it is difficult to distinguish any sort of coherent activation pattern. However at the larger values of FWHM it is much clearer to see how smoothing highlights activation signals. Nevertheless, the larger values can also show how much spatial resolution is lost from the data. The bigger values of FWHM are not in keeping with the complex shape of the brain. The clusters expand over gyri and sulci to an extent which is illogical given our understanding of the brain. In the alternative spatial smoothing techniques mentioned, the edge preservation characteristics would prevent this blurring across anatomical regions. By visualising varying values of FWHM it appears that an in-between of 3mm is an appropriate parameter for FWHM as it has removed a large portion of the

brain, exposing activation patterns, however it is still loyal to the topology of the brain. Understanding this change allows further comprehension into the delicate impact spatial smoothing has on fMRI datasets.

4.2 Implications of Results

These findings present a more nuanced understanding of the effect that spatial smoothing has on fMRI data. The overall effect is intuitive, more blurring means larger clusters, less noise and stronger activation signals, less spatial resolution. However conducting this study allowed for a deeper insight into how much affect spatial smoothing has at different levels. From the data, it seems there is a saturation effect happening, seen from both the cluster sizes and statistics, but also from the dice coefficients. This saturation leads to the idea that there is an optimal smoothing level that researchers can use when processing their data. This optimal level of spatial smoothing will remove enough noise to enhance the true activation signals, but also not distort the space in which they exist.

The broader implications of this study extend beyond technical considerations impacting our understanding of brain function and connectivity. Accurate interpretation of fMRI data is essential for advancing knowledge in both basic and clinical neuroscience. Variations in spatial smoothing can lead to different interpretations of brain activity patterns, potential affecting diagnoses and treatment plans in clinical settings. For example, the an over representation of activation patterns could impact the understanding of neurological disorders or cognitive functions. Therefore, establishing a way to optimise spatial smoothing practices is essential not only for research, but also for clinical applications where precise brain mapping is key.

Given that FWHM can affect statistical analysis and interpretation, it is crucial for researchers to be transparent about the spatial smoothing parameters they use. While there is some evidence suggesting that a more conservative approach—potentially avoiding smoothing altogether—might be beneficial (Alakörkkö et al., 2017), this is often impractical. Spatial smoothing remains a critical preprocessing step, especially in large-scale studies involving multiple participants. The challenge lies in finding the right balance: each study may require a tailored spatial smoothing approach, and clear reporting of these parameters is essential for ensuring robust and reproducible scientific findings.

The role of spatial smoothing in fMRI analysis is crucial, particularly when addressing anatomical variability across participants. Larger FWHM values, while facilitating group-level analysis by mitigating individual differences, can also obscure fine details and lead to generalisation across populations. This balance between noise reduction and spatial specificity is well-documented in the literature. For instance, Tench et al. (2014) highlighted that using a fixed FWHM can distort group-level conclusions by either diminishing small clusters in studies with fewer participants or merging clusters excessively in studies with larger samples. Their approach to dynamically adjusting FWHM based on the number of studies reflects an effort to overcome these limitations and improve accuracy.

The findings of Eickhoff et al. (2009) further emphasise the need for a more nuanced approach to spatial smoothing. Their work revealed that a fixed FWHM parameter could introduce subjectivity and inconsistencies, affecting the validity and generalisability of results. They proposed an adaptive FWHM method tailored to the empirical data, which enhanced the precision of activation likelihood estimation (ALE) and reduced false positives. This data-driven approach, in contrast to manual or fixed FWHM methods, ensures that spatial smoothing is more aligned with the actual variability and complexity of the data. This advancement shows the importance of incorporating adaptive techniques to enhance the reliability of fMRI analyses.

Researchers should stay informed about the latest developments in preprocessing methodologies and software updates to ensure that their analyses are both accurate and efficient. Embracing new technolo-

gies and methods can help mitigate the challenges associated with spatial smoothing and improve the reliability of fMRI research outcomes.

A potential technique to finding a spatial smoothing value would be to systematically vary the level before selecting one. Then comparisons can be made and the most appropriate level could be chosen. This would mean that for a variety of situations and datasets, the most appropriate level of FWHM can be chosen and the extent to which it changes the data is appreciated.

4.3 Limitations of the Study

There are limitations to this study however, the small sample size will not mimic the individual differences inherent to a larger scale study, so the level of spatial smoothing studies was much smaller. The extent of spatial smoothing might be greater, or smaller for larger scale studies. Whilst the results of this study must be interpreted with caution, researchers must still take away an understanding and appreciation for how spatial smoothing can change the results of a dataset. Another potential limitation is the preprocessing steps taken. Whilst this study was aimed at exposing how spatial smoothing alone affects the data, using FWHM alongside other processing tool may further affect its impact.

The study used cluster-based thresholding as stated in the methodology where significant clusters are identified through both voxel-wise Z-state threshold and a cluster level significance threshold ($p < 0.05$). This method is routinely used within fMRI to allow control for multiple comparisons and is more robust against noise than voxel wise thresholding alone (Woo et al., 2014). Nevertheless, it is still affected by the choice of threshold and connectivity criteria. Other methods more sensitive to noise such as k-means or GMM would potentially require a higher FWHM to distort the noise, whilst more resilient techniques such as DBSCAN or a PCA-based clustering method might suffice with a smaller FWHM.

4.4 Further Research

Further research within this area should build upon these findings by exploring ways to find optimal levels of spatial smoothing within various datasets and contexts. Conducting studies with larger sample sizes will allow more generalisation of the effects of spatial smoothing and allows investigations into how different preprocessing techniques interact with each other. Additionally, developing and validating new methodologies for determining the ideal level of spatial smoothing could enhance the accuracy of fMRI analysis. Research should also consider the impact of spatial smoothing on various types of fMRI analysis, such as task-based versus resting state studies, to provide comprehensive guidelines for different research scenarios.

4.5 Conclusion

To conclude, this study has demonstrated how spatial smoothing significantly impacts the statistical analysis and interpretation of fMRI data, affecting cluster size, activation peaks, and descriptive statistics. Even a 1mm increase or decrease in FWHM can dramatically alter the clusters' characteristics, potentially obscuring the comparability of results across studies. While it may not produce entirely different findings, inappropriate smoothing can blur complex data and generalise activation patterns across brain regions, leading to a misrepresentation of cognitive processes. This issue is well-documented in the literature, and researchers must exercise caution when comparing their findings with previous studies, particularly considering the level of spatial smoothing. The challenge of balancing signal-to-noise reduction and maintaining spatial specificity requires careful consideration, as improper selection of smoothing can skew results. Algorithmic approaches for choosing an appropriate smoothing level offer a promising solution, and future research should focus on refining these methods. While this study has limitations in

sample size and preprocessing steps, it underscores the importance of careful spatial smoothing in fMRI research, calling for continued exploration of optimal strategies for accurate data interpretation.

References

- Alakörkkö, T., Saarimäki, H., Gleean, E., Saramäki, J., & Korhonen, O. (2017). Effects of spatial smoothing on functional brain networks [Publisher: Wiley]. *The European Journal of Neuroscience*, 46(9), 2471. <https://doi.org/10.1111/ejn.13717>
- Ashburner, J., & Friston, K. J. (2005). Unified segmentation. *NeuroImage*, 26(3), 839–851. <https://doi.org/10.1016/j.neuroimage.2005.02.018>
- Ball, T., Breckel, T. P., Mutschler, I., Aertsen, A., Schulze-Bonhage, A., Hennig, J., & Speck, O. (2012). Variability of fMRI-response patterns at different spatial observation scales [_eprint: <https://onlinelibrary.wiley.com/doi/pdf/10.1002/hbm.21274>]. *Human Brain Mapping*, 33(5), 1155–1171. <https://doi.org/10.1002/hbm.21274>
- Bandettini, P. A., Wong, E. C., Hinks, R. S., Tikofsky, R. S., & Hyde, J. S. (1992). Time course EPI of human brain function during task activation. *Magnetic Resonance in Medicine*, 25(2), 390–397. <https://doi.org/10.1002/mrm.1910250220>
- Bartsch, A. J., Homola, G., Biller, A., Solymosi, L., & Bendszus, M. (2006). Diagnostic functional MRI: Illustrated clinical applications and decision-making. *Journal of magnetic resonance imaging: JMRI*, 23(6), 921–932. <https://doi.org/10.1002/jmri.20579>
- Borowsky, R., Esopenko, C., Gould, L., Kuhlmann, N., Sarty, G., & Cummive, J. (2013). Localisation of function for noun and verb reading: Converging evidence for shared processing from fMRI activation and reaction time. *Language and Cognitive Processes*, 28(6), 789–809. <https://doi.org/10.1080/01690965.2012.665466>
- Buxton, R. B., Wong, E. C., & Frank, L. R. (1998). Dynamics of blood flow and oxygenation changes during brain activation: The balloon model. *Magnetic Resonance in Medicine*, 39(6), 855–864. <https://doi.org/10.1002/mrm.1910390602>
- Cox, R. W., Chen, G., Glen, D. R., Reynolds, R. C., & Taylor, P. A. (2017). FMRI Clustering in AFNI: False-Positive Rates Redux [Publisher: Mary Ann Liebert, Inc., publishers]. *Brain Connectivity*, 7(3), 152–171. <https://doi.org/10.1089/brain.2016.0475>
- Dehghani, A., Soltanian-Zadeh, H., & Hosseini-Zadeh, G.-A. (2023). Neural modulation enhancement using connectivity-based EEG neurofeedback with simultaneous fMRI for emotion regulation. *NeuroImage*, 279, 120320. <https://doi.org/10.1016/j.neuroimage.2023.120320>
- Dice, L. R. (1945). Measures of the Amount of Ecologic Association Between Species. *Ecology*, 26(3), 297–302. <https://doi.org/10.2307/1932409>
- Dubes, R. C. (1987). How many clusters are best? - An experiment. *Pattern Recognition*, 20(6), 645–663. [https://doi.org/10.1016/0031-3203\(87\)90034-3](https://doi.org/10.1016/0031-3203(87)90034-3)
- Dymarkowski, S., Sunaert, S., Van Oostende, S., Van Hecke, P., Wilms, G., Demaerel, P., Nuttin, B., Plets, C., & Marchal, G. (1998). Functional MRI of the brain: Localisation of eloquent cortex in focal brain lesion therapy. *European Radiology*, 8(9), 1573–1580. <https://doi.org/10.1007/s003300050589>
- Eickhoff, S. B., Laird, A. R., Grefkes, C., Wang, L. E., Zilles, K., & Fox, P. T. (2009). Coordinate-based activation likelihood estimation meta-analysis of neuroimaging data: A random-effects approach based on empirical estimates of spatial uncertainty. *Human Brain Mapping*, 30(9), 2907–2926. <https://doi.org/10.1002/hbm.20718>

- Eklund, A., Nichols, T., & Knutsson, H. (2016). Can parametric statistical methods be trusted for fMRI based group studies? [arXiv:1511.01863 [math, stat]]. *Proceedings of the National Academy of Sciences*, 113(28), 7900–7905. <https://doi.org/10.1073/pnas.1602413113>
- Eklund, A., Nichols, T. E., & Knutsson, H. (2016). Cluster failure: Why fMRI inferences for spatial extent have inflated false-positive rates. *Proceedings of the National Academy of Sciences of the United States of America*, 113(28), 7900–7905. <https://doi.org/10.1073/pnas.1602413113>
- Fox, C. J., Iaria, G., & Barton, J. J. (2009). Defining the face processing network: Optimization of the functional localizer in fMRI [eprint: <https://onlinelibrary.wiley.com/doi/pdf/10.1002/hbm.20630>]. *Human Brain Mapping*, 30(5), 1637–1651. <https://doi.org/10.1002/hbm.20630>
- Friston, K. J., Williams, S., Howard, R., Frackowiak, R. S., & Turner, R. (1996). Movement-related effects in fMRI time-series. *Magnetic Resonance in Medicine*, 35(3), 346–355. <https://doi.org/10.1002/mrm.1910350312>
- Gawryluk, J. R., Mazerolle, E. L., & D'Arcy, R. C. N. (2014). Does functional MRI detect activation in white matter? A review of emerging evidence, issues, and future directions. *Frontiers in Neuroscience*, 8. <https://doi.org/10.3389/fnins.2014.00239>
- Jenkinson, M., Bannister, P., Brady, M., & Smith, S. (2002). Improved optimization for the robust and accurate linear registration and motion correction of brain images. *NeuroImage*, 17(2), 825–841. [https://doi.org/10.1016/s1053-8119\(02\)91132-8](https://doi.org/10.1016/s1053-8119(02)91132-8)
- Kanwisher, N., McDermott, J., & Chun, M. M. (1997). The Fusiform Face Area: A Module in Human Extrastriate Cortex Specialized for Face Perception. *The Journal of Neuroscience*, 17(11), 4302–4311. <https://doi.org/10.1523/JNEUROSCI.17-11-04302.1997>
- Kwong, K. K., Belliveau, J. W., Chesler, D. A., Goldberg, I. E., Weisskoff, R. M., Poncelet, B. P., Kennedy, D. N., Hoppel, B. E., Cohen, M. S., & Turner, R. (1992). Dynamic magnetic resonance imaging of human brain activity during primary sensory stimulation. *Proceedings of the National Academy of Sciences of the United States of America*, 89(12), 5675–5679. <https://doi.org/10.1073/pnas.89.12.5675>
- Liu, P., Calhoun, V., & Chen, Z. (2017). Functional overestimation due to spatial smoothing of fMRI data. *Journal of Neuroscience Methods*, 291, 1–12. <https://doi.org/10.1016/j.jneumeth.2017.08.003>
- Logothetis, N. K., Pauls, J., Augath, M., Trinath, T., & Oeltermann, A. (2001). Neurophysiological investigation of the basis of the fMRI signal. *Nature*, 412(6843), 150–157. <https://doi.org/10.1038/35084005>
- Mikl, M., Mareček, R., Hluštík, P., Pavlicová, M., Drastich, A., Chlebus, P., Brázdil, M., & Krupa, P. (2008). Effects of spatial smoothing on fMRI group inferences. *Magnetic Resonance Imaging*, 26(4), 490–503. <https://doi.org/10.1016/j.mri.2007.08.006>
- Mougin, O. E., Coxon, R. C., Pitiot, A., & Gowland, P. A. (2010). Magnetization transfer phenomenon in the human brain at 7 T. *NeuroImage*, 49(1), 272–281. <https://doi.org/10.1016/j.neuroimage.2009.08.022>
- Newton, A. T., Rogers, B. P., Gore, J. C., & Morgan, V. L. (2012). Improving measurement of functional connectivity through decreasing partial volume effects at 7 T. *NeuroImage*, 59(3), 2511–2517. <https://doi.org/10.1016/j.neuroimage.2011.08.096>
- Ogawa, S., Tank, D. W., Menon, R., Ellermann, J. M., Kim, S. G., Merkle, H., & Ugurbil, K. (1992). Intrinsic signal changes accompanying sensory stimulation: Functional brain mapping with magnetic resonance imaging. *Proceedings of the National Academy of Sciences of the United States of America*, 89(13), 5951–5955. <https://doi.org/10.1073/pnas.89.13.5951>
- Passarotti, A. M., Paul, B. M., Bussiere, J. R., Buxton, R. B., Wong, E. C., & Stiles, J. (2003). The development of face and location processing: An fMRI study. *Developmental Science*, 6(1), 100–117. <https://doi.org/10.1111/1467-7687.00259>

- Perona, P., & Malik, J. (1990). Scale-space and edge detection using anisotropic diffusion. *IEEE Transactions on Pattern Analysis and Machine Intelligence*, 12(7), 629–639. <https://doi.org/10.1109/34.56205>
- Poldrack, R. A., Mumford, J. A., & Nichols, T. E. (2011, August). *Handbook of Functional MRI Data Analysis* (1st ed.). Cambridge University Press. Retrieved August 19, 2024, from <https://www.cambridge.org/core/product/identifier/9780511895029/type/book>
- Rauch, A., Rainer, G., Augath, M., Oeltermann, A., & Logothetis, N. K. (2008). Pharmacological MRI combined with electrophysiology in non-human primates: Effects of Lidocaine on primary visual cortex. *NeuroImage*, 40(2), 590–600. <https://doi.org/10.1016/j.neuroimage.2007.12.009>
- Rombouts, S. A., Barkhof, F., Hoogenraad, F. G., Sprenger, M., Valk, J., & Scheltens, P. (1997). Test-retest analysis with functional MR of the activated area in the human visual cortex. [Publisher: American Journal of Neuroradiology]. *American Journal of Neuroradiology*, 18(7), 1317–1322. Retrieved September 18, 2024, from <https://www.ajnr.org/content/18/7/1317>
- Schilling, K. G., Li, M., Rheault, F., Gao, Y., Cai, L., Zhao, Y., Xu, L., Ding, Z., Anderson, A. W., Landman, B. A., & Gore, J. C. (2023, February). Whole-brain, gray and white matter time-locked functional signal changes with simple tasks and model-free analysis. <https://doi.org/10.1101/2023.02.14.528557>
- Seghier, M. L. (2018). Clustering of fMRI data: The elusive optimal number of clusters. *PeerJ*, 6, e5416. <https://doi.org/10.7717/peerj.5416>
- Sladky, R., Friston, K. J., Tröbstl, J., Cunningham, R., Moser, E., & Windischberger, C. (2011). Slice-timing effects and their correction in functional MRI. *NeuroImage*, 58(2), 588–594. <https://doi.org/10.1016/j.neuroimage.2011.06.078>
- Smith, A. M., Lewis, B. K., Ruttimann, U. E., Ye, F. Q., Sinnwell, T. M., Yang, Y., Duyn, J. H., & Frank, J. A. (1999). Investigation of Low Frequency Drift in fMRI Signal. *NeuroImage*, 9(5), 526–533. <https://doi.org/10.1006/nimg.1999.0435>
- Sørensen, T. J. (1948). *A method of establishing groups of equal amplitude in plant sociology based on similarity of species content and its application to analyses of the vegetation on Danish commons*. I kommission hos E. Munksgaard. Retrieved September 18, 2024, from <https://search.library.wisc.edu/catalog/9910080625002121>
- Tench, C. R., Tanasescu, R., Auer, D. P., Cottam, W. J., & Constantinescu, C. S. (2014). Coordinate Based Meta-Analysis of Functional Neuroimaging Data Using Activation Likelihood Estimation; Full Width Half Max and Group Comparisons. *PLOS ONE*, 9(9), e106735. <https://doi.org/10.1371/journal.pone.0106735>
- Thirion, B., Varoquaux, G., Dohmatob, E., & Poline, J.-B. (2014). Which fMRI clustering gives good brain parcellations? *Frontiers in Neuroscience*, 8, 167. <https://doi.org/10.3389/fnins.2014.00167>
- Tomasi, C., & Manduchi, R. (1998). Bilateral filtering for gray and color images. *Sixth International Conference on Computer Vision (IEEE Cat. No.98CH36271)*, 839–846. <https://doi.org/10.1109/ICCV.1998.710815>
- Tong, Y., Hocke, L. M., & Frederick, B. B. (2019). Low Frequency Systemic Hemodynamic “Noise” in Resting State BOLD fMRI: Characteristics, Causes, Implications, Mitigation Strategies, and Applications. *Frontiers in Neuroscience*, 13, 787. <https://doi.org/10.3389/fnins.2019.00787>
- Wandschneider, B., & Koepp, M. J. (2016). Pharmaco fMRI: Determining the functional anatomy of the effects of medication [Publisher: Elsevier]. *NeuroImage : Clinical*, 12, 691. <https://doi.org/10.1016/j.nicl.2016.10.002>
- Weiskopf, N., Scharnowski, F., Veit, R., Goebel, R., Birbaumer, N., & Mathiak, K. (2004). Self-regulation of local brain activity using real-time functional magnetic resonance imaging (fMRI). *Journal of Physiology-Paris*, 98(4), 357–373. <https://doi.org/10.1016/j.jphysparis.2005.09.019>

- Windham, M. P. (1981). Cluster validity for fuzzy clustering algorithms. *Fuzzy Sets and Systems*, 5(2), 177–185. [https://doi.org/10.1016/0165-0114\(81\)90015-4](https://doi.org/10.1016/0165-0114(81)90015-4)
- Woo, C.-W., Krishnan, A., & Wager, T. D. (2014). Cluster-extent based thresholding in fMRI analyses: Pitfalls and recommendations. *NeuroImage*, 91, 412–419. <https://doi.org/10.1016/j.neuroimage.2013.12.058>
- Woolrich, M. W., Ripley, B. D., Brady, M., & Smith, S. M. (2001). Temporal autocorrelation in univariate linear modeling of fMRI data. *NeuroImage*, 14(6), 1370–1386. <https://doi.org/10.1006/nimg.2001.0931>
- Worsley, K. J., Marrett, S., Neelin, P., & Evans, A. C. (1996). Searching scale space for activation in PET images. *Human Brain Mapping*, 4(1), 74–90. [https://doi.org/10.1002/\(SICI\)1097-0193\(1996\)4:1<74::AID-HBM5>3.0.CO;2-M](https://doi.org/10.1002/(SICI)1097-0193(1996)4:1<74::AID-HBM5>3.0.CO;2-M)
- Worsley, K. J. (2001, November). Statistical analysis of activation images. In P. Jezzard, P. M. Matthews, & S. M. Smith (Eds.), *Functional Magnetic Resonance Imaging: An Introduction to Methods* (p. 0). Oxford University Press. <https://doi.org/10.1093/acprof:oso/9780192630711.003.0014>
- Zhou, K., Ding, S., Fu, C., & Yang, S. (2014). Comparison and Weighted Summation Type of Fuzzy Cluster Validity Indices. *INTERNATIONAL JOURNAL OF COMPUTERS COMMUNICATIONS & CONTROL*, 9(3), 370–378. <https://doi.org/10.15837/ijccc.2014.3.237>